CHALMERS
UNIVERSITY OF TECHNOLOGY

Damage does not cut it - Saturated damage in FEM modelling of metal cutting breaks the simulation but not the chip

Available online at www.sciencedirect.com

ScienceDirect

Procedia Manufacturing 51 (2020) 806–811

Procedia MANUFACTURING

www.elsevier.com/locate/procedia

30th International Conference on Flexible Automation and Intelligent Manufacturing (FAIM2021)
15-18 June 2021, Athens, Greece.

Damage does not cut it – Saturated damage in FEM modelling of metal cutting breaks the simulation but not the chip

Sampsa V.A. Laakso[a]*

[a] *Chalmers University of Technology, Gothenburg, Sweden*
* Corresponding author. Tel.: nr +358407055039 *E-mail address:* sampsal@chalmers.se

Abstract

Damage models are used in metal cutting simulations to adjust the flow stress and to enable the serrated chip formation and chip breakage. The models describe the rupture strain of the material that is a function of temperature, stress, strain and strain rate. When a damage parameter in the model reaches a critical value, the flow stress of the material decreases to a predetermined fraction. Damage models show good results in predicting the cutting forces, chip thickness and serration frequency, but using them has serious disadvantages. First, damage models describe rupture strain, that is valid in metal cutting for chip breakage, but not for damage softening or chip serration, since those are based on adiabatic shear banding. Second point, shown in this paper, when material has reached the critical damage, the saturated model doesn't perform as intended. The damage model is saturated in simulations with multiple cutting passes. The initial cut deforms the layer under the tool. The same layer is then cut during the next cutting pass. During this cut, the damage model is already saturated. The damage model issues are relevant to all machining simulations because all machining processes include the multiple cutting passes.

Keywords: Damage model; FEM; Metal cutting; Subsurface deformations

1. Introduction

Cutting experiments are often done using orthogonal setup, so the chip formation can be simplified to two dimensions. Orthogonal cutting is present in planing, flange turning and tube turning. Longitudinal turning with a cutting edge angle of 90° can be viewed as nearly orthogonal condition when the depth of the cut is larger than the tool nose radius. There are three shear zones in the chip formation where material undergoes severe plastic deformation, shown in Fig 1. The tertiary shear zone is often considered while investigating the surface integrity of the machined part. One often overlooked issue is that the tertiary shear zone returns to the process after one full pass of the tool. In turning the deformed surface returns to the process after one workpiece revolution and in milling when the second insert engages the workpiece.

Nomenclature

A	Yield strength equivalent
B	Strain hardening multiplier
C	Rate hardening multiplier
n	Strain hardening exponent
m	Thermal softening exponent
ε	Plastic strain
ε_{cut}	Strain hardening cut-off strain
$\dot{\varepsilon}$	Strain rate
$\dot{\varepsilon}_{ref}$	Reference strain rate
T_{ref}	Reference or room temperature
T_{melt}	Melting temperature
C_{crit}	critical damage value
σ^*	maximum principal stress

2351-9789
10.1016/j.promfg.2020.10.113

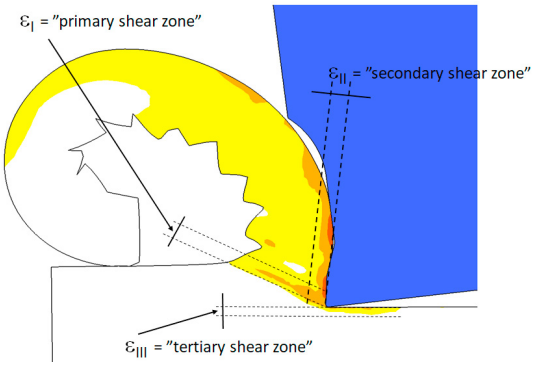

Fig 1. Shear zones in orthogonal cutting.

A major share of the research involving cutting simulations is done reduced into two dimensions, therefore the processes are presented as orthogonal cutting. In that context, it is important to note that in longitudinal cutting, in Fig 2 a), the direction of the tertiary shear zone deformation is in the direction of the feed presented with a green arrow, not in the direction of the workpiece surface presented with a red arrow. In flange turning, strains are present only in the feed direction, as shown in Fig 2 b). The experimental determination of the residual strains in the feed direction is difficult since after the spindle is stopped, the deformed layer is removed while the uncut chip thickness approaches zero. Therefore, the remaining residual strain is formed with different cutting conditions than what are present in the chip formation during the experiment. In order to experimentally determine the residual strains, a quick stop device is required. Another option is to use a broaching machine to do a single controlled pass over the workpiece.

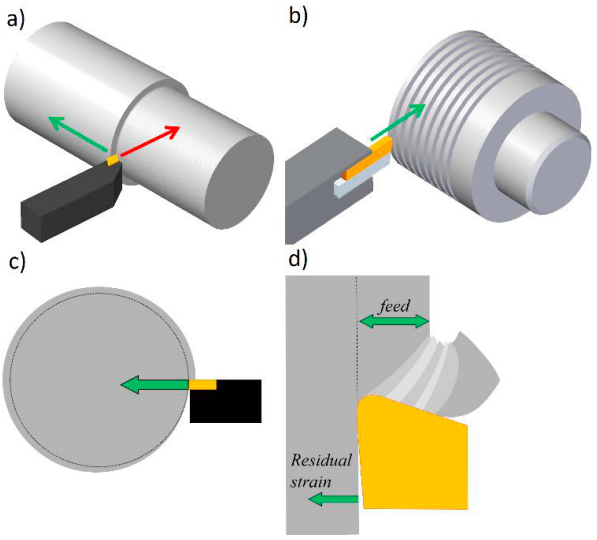

Fig 2. The direction of the residual strains in orthogonal cutting a) longitudinal turning b) flange turning c) the strain direction in flange turning d) strains in the feed direction.

There are multiple studies of surface integrity and residual stresses caused by cutting processes, and it is undisputed that cutting causes high deformation on the workpiece surface. Maranhão and Davim, 2012, concluded that cutting parameters have significant effect on residual stresses evaluated with FEM analysis. Feed and the nose radius were found to have the largest effect.[1] Ulutan and Özel in 2011 reviewed publications on Inconel and Titanium surface integrity. The results show that the workpiece surface is plastically deformed, and that the depth of the high deformation layer is about 10% of cutting feed. The subsurface deformations levelled down to base material values after 200-500 µm. Increasing the cutting speed, the cutting depth and feed increases the subsurface tensile stresses.[2]

Residual stress measurement methods can be divided into destructive and non-destructive testing, and further to surface measuring and internal measuring methods. Hole-drilling and ring-core methods are destructive methods for measuring stresses on the near surface layers. Nanoindentation is used for non-destructive surface measurements. X-ray diffraction and Barkhausen noise are non-destructive methods for internal stress measurements. Stripping and contour methods are used for destructive internal stress measurements. A common approach is to combine multiple methods for reliability and accuracy.[3]

This paper investigates the effect of the tertiary shear zone on damage model performance in FEM-modelled chip formation. The modelled case is orthogonal turning or AISI 304 stainless steel. Liu and Barash investigate the subsurface deformations in the orthogonal cutting of AISI 1018 low carbon steel. Their experiments show that the subsurface strain hardening index is 1.6 on the surface and it levels to base material values after 0.6 mm in depth. The results show interesting correlation between the shear zone length and the intensity of subsurface deformations. Increasing shear zone length leads to higher intensity deformations. Another interesting observation is that the subsurface deformations do not correlate with the extrapolated feed force at zero cutting depth. Plastic strains in magnitude between 2 to 6 mm/mm are observed in a layer reaching the depth of 0.038 mm at cutting speed 277 m/min and depth of cut 0.254 mm.[4] This also conforms with the general observation that the deformation layer is about 10% of cutting depth. Jang et al. 1996, experimented on the cutting of AISI 304 and measured residual stresses on the workpiece surface. Their results show high tensile stresses in the cutting direction and compressive stresses in the feed direction.[5] Wiesner conducted extensive cutting experiments and residual stress measurements for the orthogonal cutting of AISI 304 stainless steel using X-ray diffraction. The results show significant plastic strain in the workpiece subsurface reaching 800 µm deep into the workpiece, presented in Fig 3.[6] Yahyaoui et al. 2015 evaluated the effect of machining in the fatigue life of AISI 304 stainless steel.[7] Their results show a similar trend in the subsurface deformation distribution where the high deformation is on the surface and gradually decreasing to base material level at 600 µm depth. Based on these publications, it is evident that 304 stainless steel undergoes severe plastic deformation during machining and the depth of the deformation profile is not negligible considering the following cutting pass. The results shown in Fig 3 are representative of the results found in the literature review.

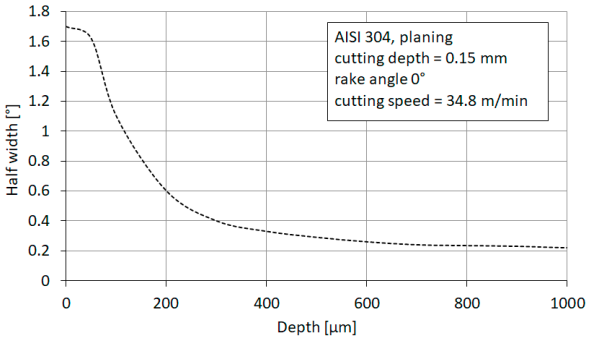

Fig 3. Subsurface deformation represented by X-ray diffraction peak half width degree profiles, modified after [6].

In order to simulate machining accurately, the subsurface deformations must be included in the model either by simulating multiple passes or defining the workpiece with initial strain distribution on the surface layer. Agmell et al. have shown that the modeling approach leads to reliable results compared with experiment values [8]. In this paper, the modelling is done by simulating multiple tool passes over the workpiece. After the first simulated cutting pass over the workpiece, the surface is left with residual stresses, heat, strains and damage. These all affect how the material behaves during the following cutting passes, but especially damage and the commonly used damage models are investigated critically. Most of the commonly used damage models like the Johnson-Cook fracture strain model or the Cockcroft-Latham damage model are based on cumulative damage value, that increases over time as a function of model specific state variables. When the damage value reaches predetermined critical value, the damage or fracture is initiated by either deleting the elements with damage or softening the flow stress using predetermined value in those elements. Damage softening can also be implemented using damage evolution, like Hillerborg's fracture energy model, where the damage softening is increased gradually instead of immediately decreasing the flow stress to a set fraction.[9] The issue with cumulative damage models is demonstrated in this paper, that when the previous cutting pass has already caused damage to the workpiece surface, the following pass will not exhibit chip serration since the material damage softening is fully saturated already at the beginning of the new cutting pass. This is true for all models based on cumulative damage value. Further criticism of the fracture-strain-based damage models is due to the chip formation mechanics, which is based on adiabatic shear banding for all non-brittle materials, not on fracturing, so using these models to simulate chip serration is physically incorrect. Another issue with cumulative damage models is mesh sensitivity [10]. The behavior of the damage model depends on the element size, as reported in [11], that affects the chip serration so that with larger element sizes, the chip serration becomes absent.

The mesh sensitivity can be corrected by using damage model with specific element length, but that only works for temperature-independent models. Larsson et al. 2015, propose using local continuum damage models combined with a scalar damage phase field, that are insensitive to mesh size. They demonstrated results with realistic ductile failure with multiple element sizes.[12] Similar methodology is used in Razanica et al. 2020 for Inconel 718 cutting simulations with overall good comparison with experiments with a relatively wide set of cutting conditions.[13] Other possible solutions to avoid the mesh dependency is to use damage models based on dynamic recrystallization like implementations of the Avrami model [14], or flow stress models with built-in strain softening, like the TANH-model [15].

2. Materials and methods

This research uses FEM-simulations to evaluate the effect of subsequent cuts in model performance and cutting experiments for reference. The experiments are done with flange turning setup with force measurement equipment and the chip thickness is measured after each experiment.

2.1. Cutting experiments

Cutting experiments are done with an SMT 500 Swedturn NC-lathe with Kistler type 9257B force sensor. Experiments are done with a solid carbide tool (WC-10%Co) with 0° rake angle and 6° clearance angle. The tool cutting edge radius is measured to be 25 µm and the initial flank wear was 30 µm in height and 70 µm in length. The cutting parameters for the experiments are v_c=140 m/min, f=0.4 mm/revolution and cutting width is 4 mm. More details about the experimental setup in [16,17].

2.2. Simulation setup

FEM software used in this paper is SFTC Deform v12.0 that uses Lagrangian formulation and a quasi-static implicit solver. The simulation was meshed with ~6500 elements, linear quadratures with four integration on the workpiece and ~1500 elements on the tool. The workpiece was modelled as an elastic-viscoplastic material and the tool as a rigid material. The workpiece mesh is refined near the tool-chip interface with element size 0.02 mm and the largest element at the bottom of the workpiece 0.2 mm. Simulation is set with 3200 timesteps of 10^{-6} s. Fig 4 shows the simulation mesh setup. The notches at the end of the workpiece are to improve iteration at the end of the simulation and to ensure clean chip removal. The simulations are done using a modified Johnson-Cook model, presented in equation *1* where the strain hardening is limited to cutoff strain.[18] The chip serration is modelled using Cockcroft-Latham damage model, shown in equation *2*.[19]

$$\sigma = \begin{cases} (A + B\varepsilon^n)\left[1 + C\,ln\left(\frac{\dot{\varepsilon}}{\dot{\varepsilon}_{ref}}\right)\right]\left[1 - \left(\frac{T - T_{ref}}{T_{melt} - T_{ref}}\right)^m\right] & if\varepsilon < \varepsilon_{cut} \\ (A + B\varepsilon_{cut}{}^n)\left[1 + C\,ln\left(\frac{\dot{\varepsilon}}{\dot{\varepsilon}_{ref}}\right)\right]\left[1 - \left(\frac{T - T_{ref}}{T_{melt} - T_{ref}}\right)^m\right] & if\varepsilon \geq \varepsilon_{cut} \end{cases} \quad (1)$$

$$C_{crit} = \int^{\varepsilon} \sigma^* d\varepsilon \quad (2)$$

The model parameters for AISI 304 stainless steel used in the simulation are presented in Table 1. Critical value of Cockcroft-Latham model was set to 130 and damage softening to 38%. Shear friction 0.6 was used between the tool and the workpiece. Elastic and thermal properties of AISI 304 are given in [20].

Table 1. Johnson-Cook model parameters.

A	B	n	C	m	T_{melt}	T_{ref}	$\dot{\varepsilon}_{ref}$	ε_{cut}
418.7	2200.5	0.594	0.07	1	1400	20	1	0.203

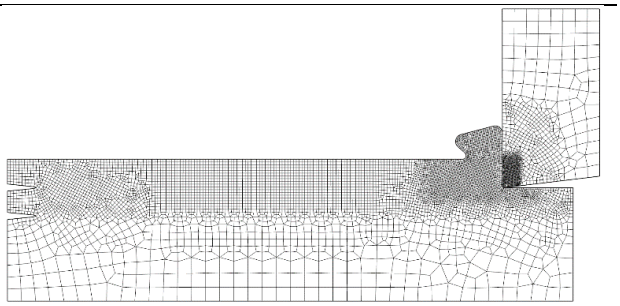

Fig 4. Simulation mesh setup.

3. Results

3.1. Cutting experiment results

Cutting experiment results are shown in Table 2. Cutting forces have relatively high standard deviation but chip thickness is stable.

Table 2. Cutting experiment results.

	Avg.	St.Dev.
F_C [N]	3047	9.8%
F_f [N]	1269	12.1%
t_c [mm]	0.77	2.2%

3.2. Simulation results

Simulation results are presented in Fig 5 to Fig 9. Fig 5 presents the strain, damage and temperature distribution after the first cutting pass. The strain distribution conforms with the results from literature review. The simulated cutting force signals are presented in Fig 6 to Fig 8. The cutting forces do not have intuitive behavior as the cutting force decreases and feed force increases during the second cutting pass. The simulation with initial damage removed, both force components increase significantly compared with the first cutting pass and the simulation error decreases regarding the cutting forces but increases regarding the chip thickness. Table 3 shows the averaged force and chip thickness and errors compared with experiments. Fig 9 shows the chip shape, serration frequency and strain distribution of the simulations. The initial subsurface deformation has significant effect on the simulation output during the second cutting pass. First, the effect of initial deformation presented in the second picture from the top in Fig 9., shows that the chip thickness decreases significantly, and chip serration is absent. This shows the shortcoming of cumulative damage models when the damage has been saturated, the model does not perform correctly. If the damage is removed from the surface as in the last picture in Fig 9, the chip is still significantly thinner, but serration is present.

Table 3 Simulated forces and chip thicknesses and corresponding errors.

	F_c [N]	F_f [N]	t_c [mm]	F_c error	F_f error	t_c error
Pass #1	2809	778	0.70	-8 %	-39 %	-9 %
Pass #2	2602	1075	0.33	-15 %	-15 %	-57 %
Pass #3	3328	1133	0.44	9 %	-11 %	-43 %
Experiment	3047	1269	0.77			

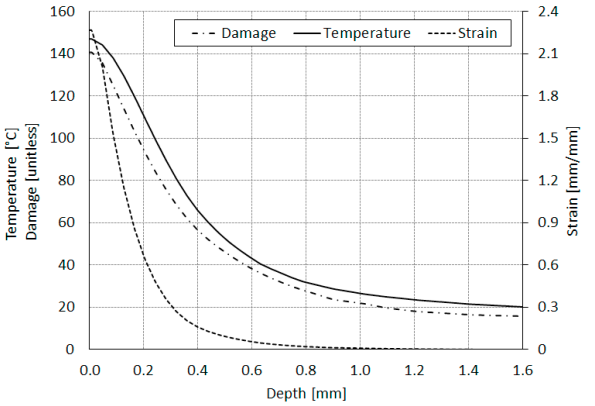

Fig 5. Strain, Damage and Temperature profiles after the first tool pass.

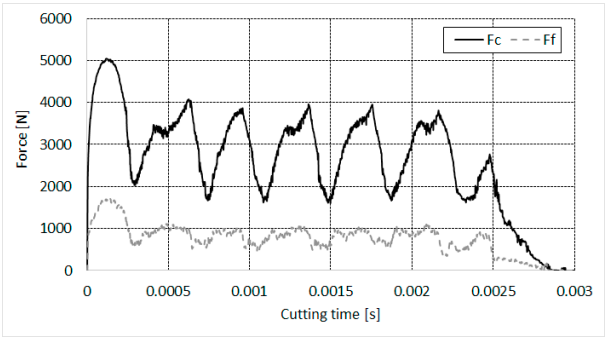

Fig 6. Cutting forces in the first cutting pass.

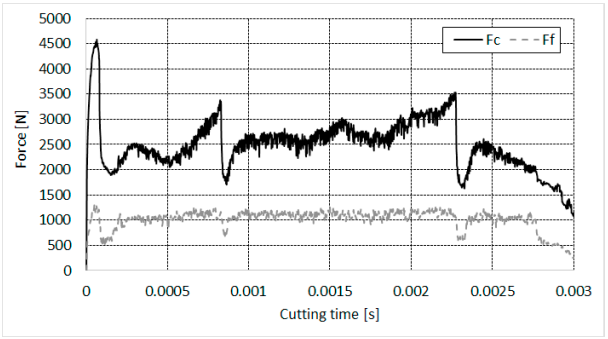

Fig 7. Cutting forces in the second cutting pass.

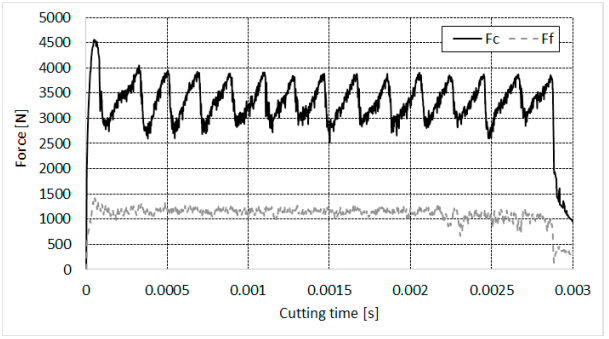

Fig 8. Cutting forces in the second cutting pass with the initial damage removed.

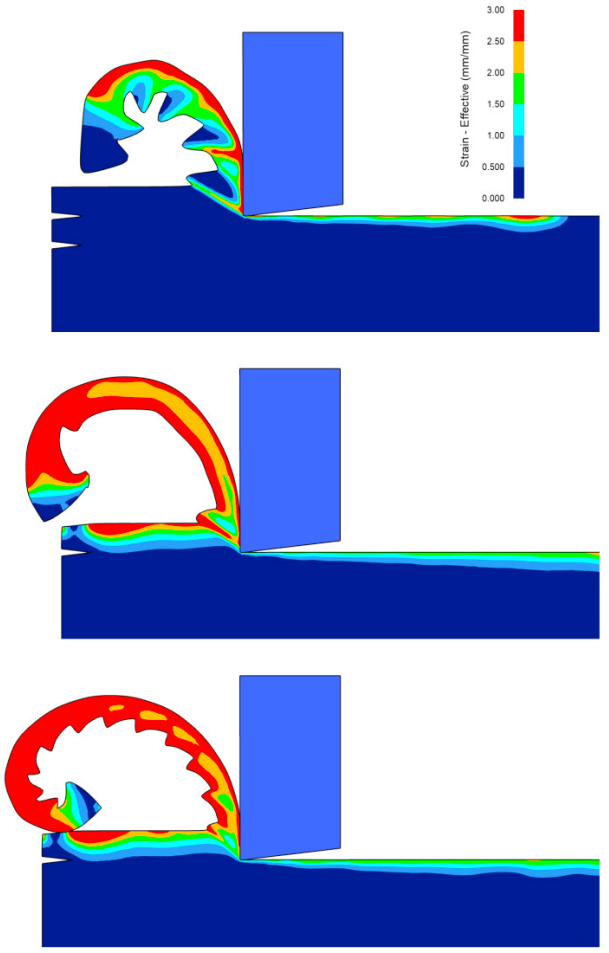

Fig 9. The simulation output and the strain distribution, top down: the first cutting pass, the second cutting pass and the second cutting pass with the initial damage removed.

4. Discussion and conclusions

This paper investigates how subsequent cuts affect the simulation of flange turning of AISI 304 stainless steel. The simulations show that the subsurface deformation, damage and temperature profiles caused by the first cut have significant effect on the following cutting pass. The simulated strain distribution was found to conform with the previous research findings in reviewed articles. The effects of the initial subsurface deformations are:

- Reduced cutting force
- Increased feed force
- Reduced chip thickness
- Absent chip serration

The absence of chip serration is caused by the damage model, which does not perform correctly when the damage is saturated on the workpiece surface. In order to avoid this, the same setup for second cutting pass was simulated with initial damage removed. When the initial damage is removed, but initial strain and temperature are left on the workpiece surface, the effects are:

- Increased cutting force
- Increased feed force
- Reduced chip thickness
- Higher chip serration frequency

These results have major consequences on metal cutting FEM simulations in general.

First, in addition to reported mesh sensitivity issues and incorrect physical assumptions regarding chip serration, these results prove another argument why damage models based on cumulative damage should be avoided.

Second, the initial subsurface strain has major effect on cutting forces and chip thickness. Material model parameters are commonly acquired using inverse methods, that use cutting forces and chip thickness as reference values. If material model parameters are acquired using inverse methods, the initial assumptions are wrong if the workpiece has not been initialized with correct strain distribution. This leads to material model parameters that can perform well in specific cutting conditions, but the parameters are not applicable if the cutting conditions change.

Finally, these results appear to be related to the feed force error, that is universally present in metal cutting FEM-simulations reported in many articles [21]. The feed force error is referred to because the simulations underestimate the feed force compared with the experiments [22]. To the author's knowledge, there has not been a single metal cutting paper where all, cutting force, feed force and chip thickness have been simulated in multiple cutting conditions without considerable (>10%) error in at least one of the listed outputs. The feed force error can be mitigated by increasing the friction coefficient, but in that case the cutting force and chip thickness are overestimated [23]. However, the results in this paper show that the initial strain increases the cutting forces and decreases the chip thickness. If the material model is calibrated with a proper set of material testing and fine-tuned with an inverse method using simulations with the initial strain distribution measured from the experiments, the qualitative effects reported in this paper imply that the feed force error would be predicted accurately with correct material model parameters and correct initial strain distribution.

5. Future Work

The results shown in this paper have significant impact on metal cutting simulations practices. Therefore, to have high confidence in the made assumptions, rigorous testing and verification of the results is needed. The following steps are required in future work:

- Experimental determination of the subsurface deformation distributions
- Experimental determination of the subsurface temperature distribution in steady state
- Implementation of more realistic damage model that doesn't have the saturation issues
- Verification of the results for multiple materials

References

[1] Maranhão C, Davim JP. Residual stresses in machining using fem analysis: A review. Rev Adv Mater Sci. 2012;30:267–72.

[2] Ulutan D, Özel T. Machining induced surface integrity in titanium and nickel alloys: A review. Int J Mach Tools Manuf [Internet]. 2011;51(3):250–80.

[3] Guo J, Fu H, Pan B, Kang R. Recent progress of residual stress measurement methods: A review. Chinese J Aeronaut [Internet]. 2019;

[4] Liu CR, Barash MM. The Mechanical State of the Sublayer of a Surface Generated by Chip-Removal Process—Part 1: Cutting With a Sharp Tool. J Eng Ind [Internet]. 1976 Nov 1;98(4):1192–9.

[5] Jang DY, Watkins TR, Kozaczek KJ, Hubbard CR, Cavin OB. Surface residual stresses in machined austenitic stainless steel. Wear [Internet]. 1996;194(1):168–73.

[6] Wiesner C. Residual stresses after orthogonal machining of AlSl 304: numerical calculation of the thermal component and comparison with experimental results. Metall Trans A [Internet]. 1992 Nov;23(3):989–96.

[7] Yahyaoui H, Ben Moussa N, Braham C, Ben Fredj N, Sidhom H. Role of machining defects and residual stress on the AISI 304 fatigue crack nucleation. Fatigue Fract Eng Mater Struct [Internet]. 2015 Apr 1;38(4):420–33.

[8] Agmell M, Ahadi A, Zhou JM, Peng RL, Bushlya V, Ståhl J-E. Modeling subsurface deformation induced by machining of Inconel 718. Mach Sci Technol [Internet]. 2017 Jan 2;21(1):103–20.

[9] Agmell M, Bushlya V, Laakso SVA, Ahadi A, Ståhl J-E. Development of a simulation model to study tool loads in pcBN when machining AISI 316L. Int J Adv Manuf Technol [Internet]. 2018;

[10] Ljustina G, Fagerström M, Larsson R. Rate Sensitive Continuum Damage Models and Mesh Dependence in Finite Element Analyses. Huespe AE, editor. Sci World J [Internet]. 2014;2014:260571.

[11] Ambati R, Yuan H. FEM mesh-dependence in cutting process simulations. Int J Adv Manuf Technol [Internet]. 2011;53(1):313–23.

[12] Larsson R, Razanica S, Josefson BL. Mesh objective continuum damage models for ductile fracture. Int J Numer Methods Eng [Internet]. 2016 Jun 8;106(10):840–60.

[13] Razanica S, Malakizadi A, Larsson R, Cedergren S, Josefson BL. FE modeling and simulation of machining Alloy 718 based on ductile continuum damage. Int J Mech Sci [Internet]. 2020;171:105375.

[14] Arısoy YM, Özel T. Prediction of machining induced microstructure in Ti–6Al–4V alloy using 3-D FE-based simulations: Effects of tool micro-geometry, coating and cutting conditions. J Mater Process Technol [Internet]. 2015 Jun;220:1–26.

[15] Calamaz M, Coupard D, Girot F. A new material model for 2D numerical simulation of serrated chip formation when machining titanium alloy Ti–6Al–4V. Int J Mach Tools Manuf [Internet]. 2008 Mar;48(3–4):275–88.

[16] Laakso SVA, Agmell M, Ståhl J-E. The mystery of missing feed force — The effect of friction models, flank wear and ploughing on feed force in metal cutting simulations. J Manuf Process [Internet]. 2018;33:268–77.

[17] Laakso SVA, Zhao T, Agmell M, Hrechuk A, Ståhl J-E. Too Sharp for its Own Good – Tool Edge Deformation Mechanisms in the Initial Stages of Metal Cutting. Procedia Manuf. 2017;11.

[18] Johnson GR, Cook WH. A constitutive model and data for metals subjected to large strains, high strain rates and high temperatures. In: Proceedings of the 7th International Symposium on Ballistics. 1983. p. 541–7.

[19] Cockcroft MG, Latham DJ. Ductility and the workability of metals. J Inst Met. 1968;96:33–9.

[20] Laakso SVA. Heat matters when matter heats – The effect of temperature-dependent material properties on metal cutting simulations. J Manuf Process [Internet]. 2017 Jun;27:261–75.

[21] Eck S, Gänser H-P, Marsoner S, Ecker W. Error Analysis for Finite Element Simulation of Orthogonal Cutting and its Validation Via Quick Stop Experiments. Mach Sci Technol [Internet]. 2015 Jul 3;19(3):460–78.

[22] Nasr MNA, Ammar MMA. An Evaluation of Different Damage Models when Simulating the Cutting Process Using FEM. Procedia CIRP [Internet]. 2017;58:134–9.

[23] Malakizadi A, Hosseinkhani K, Mariano E, Ng E, Del Prete A, Nyborg L. Influence of friction models on FE simulation results of orthogonal cutting process. Int J Adv Manuf Technol [Internet]. 2017;88(9):3217–32.